

CHARGED PARTICLE PRODUCTION  
AT THE FERMILAB COLLIDER DETECTOR

Virgil E. Barnes  
Purdue University  
West Lafayette, Indiana 47906  
USA  
(Representing the CDF Collaboration<sup>\*</sup> )



**ABSTRACT**

Results are presented on minimum-bias inelastic events from 1987 data for  $\bar{p}p$  collisions at 1.8 and 0.63 TeV center of mass energy, and are compared with data at lower energy and with data from the C0 experiment. Transverse momentum spectra harden as the center of mass energy  $\sqrt{s}$  increases, and a QCD-inspired parton model with fragmentation functions is in qualitative agreement with the data over a very wide range of  $\sqrt{s}$  and  $p_T$ . The mean transverse momentum of charged particles increases faster than linearly with  $\ln(s)$ . Between 630 and 1800 GeV this increase is dominated by charged particles having  $p_T$  less than about 3 GeV/c. Charged particles frequently form clusters having a cluster transverse energy greater than a few GeV. Events having at least one such cluster in the rapidity range  $|\eta| < 0.7$  have mean multiplicity twice as large as the conjugate sample of non-cluster events. Events with clusters also show a substantial change in multiplicity between 630 and 1800 GeV, whereas non-cluster events show little variation with  $\sqrt{s}$ .

\* ANL-Brandeis-University of Chicago- Fermilab-INFN, Frascati-Harvard-University of Illinois-KEK-LBL-University of Pennsylvania-INFN, University and Scuole Normale, Pisa-Purdue-Rockefeller-Rutgers-Texas A&M-Tsukuba-University of Wisconsin

## 1. INTRODUCTION

The Tevatron Collider at Fermilab permits the study of hadronic collisions at center of mass energies up to  $\sqrt{s} = 1.8$  TeV. Data on charged particle production relating to hardening of the inelastic minimum-bias-trigger events with  $\sqrt{s}$  are presented, as outlined in the above abstract.

The Collider Detector at Fermilab (CDF) is a large, general purpose azimuthally symmetric  $4\pi$  detector covering polar angles from  $2^\circ$  to  $178^\circ$  with respect to the collision axis, corresponding to a range of pseudorapidity  $-4 < \eta < 4$  [ $\eta = \ln(\tan(\theta/2))$ ]. CDF has high resolution tracking in a 1.5 T magnetic field followed by fine-grained projective tower calorimeters, and then by muon tracking over portions of the above range of  $\eta$ . The detector has been described in detail elsewhere<sup>1)</sup>. It is well suited to studying individual charged hadrons, jets, and leptons having a wide range of energies and transverse momenta. The central portions of the detector used in the present analysis, and the trigger and event selection for minimum bias events, are discussed below. Further details of the analysis can be found in Ref. 2).

## 2. THE CENTRAL TRACKING DETECTORS

The present minimum bias data analysis uses charged tracks found in the Vertex Time Projection Chamber (VTPC)<sup>3)</sup> or in the Central Track Chamber (CTC)<sup>4)</sup> (Fig. 1).

The VTPC covers a range  $|\eta| < 3.5$ , with full acceptance for  $|\eta| < 3.0$ . It is discussed in detail in the accompanying report on charged particle multiplicities, by F. Snider.<sup>5)</sup>

The CTC is a large drift chamber with inner radius 0.3 m and outer radius 1.3 m. Sense wires are arranged in 5 axial superlayers of 12 layers each, and 4 small-angle stereo ( $\pm 3^\circ$ ) superlayers of 6 layers each, with full geometrical acceptance up to  $|\eta| = 1$  and full 3-dimensional reconstruction well beyond that point. Coverage is complete in azimuth. The transverse momentum resolution, including both single hit resolution and multiple scattering, was  $\sigma_{p_T}/p_T^2 \leq 0.003$  GeV $^{-1}$  for  $|\eta| \leq 1.0$ . The CTC data permit reconstruction of over 100 tracks in events with high local track density. The CTC has  $>99\%$  efficiency for tracks with  $p_T > 400$  MeV/c and  $|\eta| < 1.0$ ; only CTC tracks passing these two cuts are used in the present analysis.

## 3. TRIGGER AND EVENT SELECTION

Scintillator hodoscopes (Fig. 1) located at Z (along the beam) =  $\pm 5.82$  m and covering the range  $3.24 < |\eta| < 5.89$  (the Beam-Beam Counters or BBC) are used to trigger on most of the inelastic cross section, and also serve as a luminosity monitor.

The minimum bias (MB) data samples were obtained with a trigger requiring that at least one charged particle traverse each set of BBC, in coincidence with the beam crossing. At  $\sqrt{s} = 1.8$  TeV (630 GeV), 55,700 (9,400) triggers were analyzed. Beam-beam collision events were selected by requiring that (a) at least 4 charged particles were found in the VTPC in the range  $-3 < \eta < 3$  and at least one of these tracks be in each hemisphere ( $\eta > 0$  and  $\eta < 0$ ), and (b) the Z of the vertex from BBC timing agreed within 16 cm with  $Z_{VTPC}$  determined from VTPC tracks.

The Beam-Beam event vertices were distributed in Z with a Gaussian  $\sigma_z$  typically  $\sim 40$  cm. To ensure uniform VTPC track acceptance, we also required  $|Z_{VTPC}| < 65$  cm. After these cuts, the contamination of non-beam-beam events was estimated to be less than 2.5% in the single low-luminosity 630 GeV run, and less than 0.5% at 1.8 TeV, where the typical luminosity was up to  $4 \times 10^{28}$  cm $^{-2}$ sec $^{-1}$  for MB runs. The final MB sample consists of 44,300 (3,800) events at the two energies.

The effective BBC trigger cross section was estimated by extrapolating the **total** and elastic cross sections to 1.8 TeV, giving  $77 \pm 6$  mb and  $17.6 \pm 1.6$  mb, respectively. The  $\sim 60$  mb of inelastic cross section is divided into single diffractive (SD), double diffractive (DD), and non diffractive (ND) events. The acceptances ( $\epsilon$ ) of the BBC were found by Monte Carlo simulation and are 96% (93%) for ND, 57% for DD, and 16% (11%) for SD events at 1800 (630) GeV. Using a recent UA4 measurement<sup>6)</sup> of  $\sigma_{SD} = 9.4 \pm 0.7$  mb at 546 GeV, and its extrapolation to 1800 GeV, we estimate that the effective trigger cross sections,  $\sigma_{eff}$ , are  $43 \pm 6$  mb and  $34 \pm 3$  mb, respectively.

Since  $\sigma_{DD}$  is estimated to be a few mb, the CDF MB sample is dominantly non-diffractive inelastic events, with a few millibarns contamination of high mass SD and DD events.

#### 4. TRANSVERSE MOMENTUM DISTRIBUTIONS AND $\langle p_T \rangle$

The charged particle invariant cross section is defined as:

$$Ed^3\sigma/d^3p = (\sigma_{eff}/N_{evt})(N/p_T \cdot \Delta p_T \cdot \Delta\phi \cdot \Delta y)$$

where  $N_{evt}$  is the number of events used and  $N$  is the number of charged tracks in a given element of phase space. The invariant cross sections as a function of  $p_T$  for the CDF data are shown in Ref. 2. The 630 GeV data are measured up to 3.5 GeV/c and are in good agreement with the UA1 and UA2 data<sup>7)</sup> at 546 GeV. The data at 1.8 TeV extend to  $p_T = 10$  GeV/c, and fall less rapidly with  $p_T$  than the 630 GeV data, being a factor of 4 higher at 3.5 GeV/c. Invariant cross sections were fitted to a parton-model-inspired power law

$$Ed^3\sigma/d^3p = A \frac{p_o^n}{(p_T + p_o)^n}$$

The parameters  $p_o$  and  $n$  are highly correlated and good fits can be obtained with a change in  $n$  compensating a change in  $p_o$ . We fix  $p_o = 1.3$  GeV/c as is done at lower  $\sqrt{s}$ . (When  $p_o$  is left free, the fit at 1.8 TeV gives  $p_o = 1.29$ ). Values of  $n$  decrease with increasing  $s$ : UA1 (546 GeV)  $n = 9.14 \pm 0.02$ ; CDF (630 GeV)  $n = 8.89 \pm 0.06$ ; CDF (1.8 TeV)  $n = 8.28 \pm 0.02$ , reflecting the hardening of the  $p_T$  spectrum with rising  $s^2$ .

Fig. 2 shows the CDF 1.8 TeV data, together with the UA1 data, ISR data (British Scandinavian) and Fermilab fixed target data (Chicago Princeton). (See also Ref. 2 and references therein.) The 1.8 TeV data fall much less steeply with  $p_T$ , being 5 orders of magnitude larger than the 27 GeV data at  $p_T = 7$  GeV/c.

A calculation by S. Ellis and J. Stirling<sup>8)</sup>, based on the parton model and QCD, attempts to calculate the inclusive charged particle  $p_T$  spectra for  $\sqrt{s}$  ranging from fixed target energies up to Tevatron collider energies. The ingredients are (a) structure functions  $F(x, Q^2)$  for two colliding partons, one in the proton and one in the anti-proton (or other proton) determined from experiment and from QCD evolution in Bjorken  $x$ , (b) fragmentation functions  $D(z)$  for production of various hadrons, again determined from experiment, and (c) a QCD parton-parton scattering cross section  $\hat{\sigma}(\hat{s}, \hat{t}, \hat{u})$ . Fig. 2 also shows the results of the calculations, using Duke and Owens set 1 structure functions with  $Q^2 = p_T^2$  and a K-factor of 2. Compared with the data above  $p_T = 1$  GeV/c, the  $p_T$  and  $s$  dependences agree, within a factor of  $\sim 2$  to 5, over nine decades of invariant cross section and  $\sqrt{s}$  from 27 to 1800 GeV.

In determining  $\langle p_T \rangle$ , extrapolation is required for the substantial portion of the  $p_T$  spectrum below the 400 MeV/c cutoff. Alternative functional forms used include: (a) the above power law form, (b) a simple exponential  $A \exp(-bp_T)$  and (c) a polynomial  $A(p_T^2 +$

$B \cdot p_T + C$ ). Systematic uncertainties due to choice of functional form are much reduced by the powerful constraint that the area under the entire curve must be given by  $dN/d\eta$ . When the three functions are fitted to the data between 400 and 600 MeV/c, with  $dN/d\eta$  fixed, the systematic error due to the choice of functional form is reduced to 0.003 GeV/c. We use the well-determined ratio  $1.27 \pm .04$  of the  $dN/d\eta$  plateau heights at 1.8 and 0.63 TeV as determined in the VTPC<sup>5</sup>) (This ratio is slightly higher than the value 1.22 - 1.25 predicted by the Dual Parton Model<sup>9</sup>), or the value 1.20 predicted by the Lund-PYTHIA Monte Carlo program<sup>10</sup>.) We also fix  $dN/d\eta = 3.30 \pm 0.15$  at 630 GeV by interpolating measurements in the range 200 to 900 GeV<sup>11</sup>). We then obtain  $\langle p_T \rangle = 0.495 \pm 0.014$  ( $0.432 \pm 0.004$ ) GeV/c at 1.8 (0.63) TeV. There is an additional common uncertainty of 0.020 GeV/c in both numbers due to the 5% uncertainty in  $dN/d\eta$  at 630 GeV. The C0 experiment at 1.8 TeV quotes  $\langle p_T \rangle = 0.47 \pm 0.01$ <sup>12</sup>). This value and the CDF value at 1.8 TeV are in good statistical agreement.

Fig. 3 shows  $\langle p_T \rangle$  as a function of  $\sqrt{s}$  which rises substantially faster than  $\ln(s)$ . The common uncertainty of the two CDF points is omitted, and will not affect the slope from 0.63 to 1.8 TeV, which is clearly steeper than at lower  $\sqrt{s}$ .

Although the rise with  $s$  of the high  $p_T$  tail of the particle spectrum is striking, the value of  $\langle p_T \rangle$  is largely determined by particles with  $p_T < 3$  GeV/c, as seen in Fig. 4a. The ratio of the  $\langle p_T \rangle$  values at the two CDF energies has risen half way between 1.0 and its asymptotic value of 1.27, using tracks below 0.8 GeV/c, as seen in Fig. 4b. Using tracks below 3 GeV/c gives a ratio within a few percent of that obtained using all tracks.

## 5. CHARGED PARTICLE CORRELATIONS AND CLUSTERING

A tendency is seen for charged CTC tracks to cluster in  $\eta$  and  $\phi$  around high  $p_T$  tracks. Figs. 5a,b and c show the charged particle transverse momentum flow around "trigger" particles having various ranges of  $p_T$ . The distributions exclude the  $p_T$  of the trigger particle. Fig. 5a shows  $d\Sigma p_T/d\Delta\eta$  as a function of distance in pseudorapidity from the trigger particle, for "same-side" tracks having  $\Delta\phi$  within  $90^\circ$  of the trigger particle. There is clear peaking around the trigger particle, which becomes more pronounced for larger trigger  $p_T$ . Fig. 5b shows a strong tendency for momentum density  $d\Sigma p_T/d\Delta\phi$  to peak both in the direction of the trigger particle and also at  $\Delta\phi = 180^\circ$  opposite to the trigger particle. Fig. 5c is for away-side tracks, in the  $\phi$  semicircle opposite to the trigger particle. No  $\eta$  correlation is seen.

The same patterns are seen, but are much more pronounced, in samples of high  $p_T$  jet events (not shown) which were selected using a central calorimeter jet trigger and which are clearly dominated by two-jet events. The absence (presence) of away-side correlations in  $\eta$  ( $\phi$ ) in the high  $p_T$  jet sample can be understood in terms of parton-parton collisions with small overall  $p_T$  and conservation of  $p_T$ , and with a wide spread of overall longitudinal momentum,  $p_Z$ , reflecting the  $x$  distributions of the colliding partons.

The patterns of Fig. 5 are suggestive of the charged portion of low- $p_T$  jets. This further motivates a search for charged clusters using an algorithm similar to calorimeter transverse energy  $E_T$  clustering algorithms used to find jets. Using charged tracks has certain advantages over calorimeter clustering at low  $p_T$ : (a) track momentum resolution  $\sigma_{p_T}/p_T$  is less than 2.5% for the MinBias event sample, (b) track directions at the primary vertex are used, whereas low momentum tracks are swept by the magnetic field to the wrong azimuth at the calorimeter and (c) the hadron calorimeter response is known to be nonlinear at low  $E_T$ . Disadvantages of clustering only charged tracks include: (a) on average, one-third or more of the hadronic energy is expected to be in neutral particles and (b) event-to-event

fluctuations in the neutral to charged energy ratio will smear the cluster energy estimate. An attempt is being made to include neutral particles by incorporating transverse energy seen in the central electromagnetic calorimeters, with a correction for energy deposited in the calorimeter by charged tracks. Only the charged particle cluster analysis will be shown here; but events with possible calorimeter noise have been removed and the sample used is some 36,000 (3,800) events at 1800 and 630 GeV.

A charged cluster is defined as a set of tracks having rapidity  $y > y_o = 1.0$  along a common axis. This corresponds roughly to a cone of half angle  $40^\circ$ , or to a radius  $R < 0.7$  in  $\eta - \phi$  space. The search starts with the axis along the highest- $p_T$  track, and iteratively adjusts the cone axis as the cluster is formed. All particles not yet in a cluster are used in descending  $p_T$  as cluster seeds, with no threshold in  $p_T$ . Each cluster's transverse energy is then calculated:

$$E_T^{clust} = [(\sum E_i)^2 - (\sum P_{zi})^2]^{1/2}$$

where the  $E_i$  are calculated using the pion mass.

The  $E_T^{clust}$  spectra for clusters with  $|\eta| < 0.7$  are shown in Fig. 6 for 1.8 TeV and 630 GeV minimum bias events. The spectrum is seen to harden as  $\sqrt{s}$  increases, with a factor of 4 rise for  $E_T^{clust} \sim 7$  to 10 GeV. These charged clusters occur quite copiously, with 35 to 40% probability per MinBias event for  $1 \leq E_T^{clust} \leq 2$  GeV. At 1.8 TeV the integrated probability of a cluster with  $E_T^{clust} > 3$  GeV in the central 1.4 units of  $\eta$  is 11% per event. One should be cautious in interpreting clusters of such low  $E_T$ , where the applicability of perturbative QCD is not clear. Further caveats are in order because of the possible inclusion of underlying event energy in the clusters, and the omission of neutral energy in the present analysis.

We divide the minimum bias events into two classes: those having at least one central cluster with  $|\eta_{cluster}| < 0.7$  and  $E_T^{clust} > 3$  GeV; and all other MinBias events. We repeat the division using  $E_T^{clust} > 1$  GeV to define cluster events. Table 1 gives the mean charged multiplicities (as measured in the VTPC with  $|\eta| < 3.0$ ) for the cluster and non-cluster event samples at 1800 and 630 GeV.

Table 1.  $\langle N_c \rangle$  (VTPC) for cluster and non-cluster events.

<i>EventClass</i> :	3 GeV Clust.	Non-Clust.	1 GeV Clust.	Non-Clust.
$\sqrt{s} = 1800$ GeV	$60.3 \pm 31$	$27.8 \pm 10$	$41.1 \pm 14$	$18.8 \pm 09$
$\sqrt{s} = 630$ GeV	$49.0 \pm 1.1$	$24.1 \pm .22$	$33.1 \pm .36$	$18.2 \pm .23$

The ratio of mean charged multiplicity for cluster events/non-cluster events is within 10% of 2.0 in all cases, and grows either with  $s$  or with the  $E_T^{clust}$  cut. Figs. 7a and 7b show the  $N_c$  spectra for 3 GeV cluster events and non-1-GeV-cluster events, respectively, at 1.8 TeV representing typical distributions for the cluster and non-cluster samples.  $N_c$  increases by 23 – 24% between 630 and 1800 GeV for the 3 GeV and 1 GeV cluster event samples. By contrast,  $N_c$  changes very little (4%) for the non-1-GeV-cluster events. Whether this latter sample represents an underlying soft component of minimum bias events, or is an artifact of the cluster-defining algorithm, is a subject for further investigation and interpretation.

## ACKNOWLEDGEMENTS

The CDF collaboration wishes to thank the CDF technical support staff, and the staff of the TeVatron Collider, for their invaluable contributions to this experiment. This work was supported by the U.S. Department of Energy, the National Science Foundation, the Italian Istituto Nazionale di Fisica Nucleare, the Japanese Ministry of Science, Culture and Education, and the A. P. Sloan Foundation.

## REFERENCES

- 1) F. Abe et al., Nucl. Inst. Meth. A271 (1988) 387.
- 2) F. Abe et al., Phys. Rev. Lett. 61 (1988) 1819.
- 3) F. Snider et al., Nucl. Inst. Meth. A268 (1988) 75.
- 4) F. Bedeschi et al., Nucl. Inst. Meth. A268 (1988) 50.
- 5) F. Snider, Pseudorapidity Distributions of Charged Particles Produced in  $\bar{p}p$  Interactions at  $\sqrt{s} = 630$  and 1800 GeV, these proceedings.
- 6) D. Bernard et al., Phys. Lett. 186B (1987) 227.
- 7) G. J. Alner et al., Phys. Lett. 138B (1984) 304,  
G. J. Alner et al., Phys. Lett. 160B (1984) 199.
- 8) S. Ellis and W. J. Stirling, private communication.
- 9) Dual Parton Model, A. Capella, U. Sukhatme, C-I Tan, and J. Tran Thanh Van, Multiparticle Production, ed. P. Carruthers (World Scientific, 1988); ratio is from a Monte Carlo program made available by J. Tran Thanh Van. For an extension of the DPM to include hard parton collisions, see J. Ranft et al., SSC Central Design Group report SSC-149 (December, 1987); ratio is from a Monte Carlo calculation by J. Ranft (private communication).
- 10) H-U Bengtsson and T. Sjostrand, Computer Phys. Communications 46 (1987) 43.
- 11) G. Ekspong, Nucl. Phys. A461 (1987) 145, and references therein.
- 12) C. Lindsay, Recent Results from E-735: Search for Quark Gluon Plasma in  $\bar{p}p$  Collisions at  $\sqrt{s} = 1.8$  TeV, Proceedings of the Quark Matter '88 Conference, Lenox, Mass. (to be published in Nucl. Phys.); also Phys. Rev. Letters 60 (1988) 1622 (the first reference uses a functional form to extrapolate to high  $p_T$ ; the second reference quotes a value of  $\langle p_T \rangle = 0.46, 0.01$  units lower, using tracks only up to 3 GeV/c where the C0 track momentum resolution becomes poor).

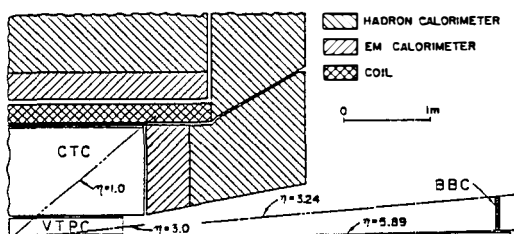


Fig. 1 A quarter-section of the central portion of the CDF detector showing the CTC, VTPC, and Beam Beam Counters.

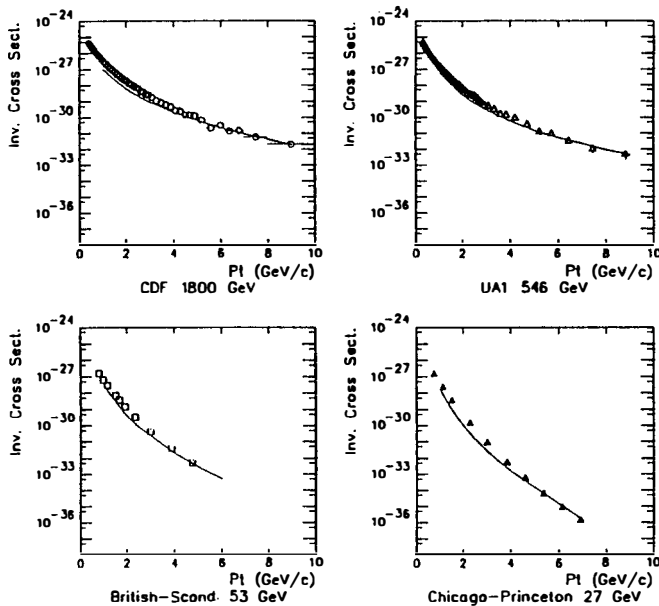


Fig. 2 Invariant cross sections  $Ed^3\sigma/d^3p(cm^2c^3/GeV^2)$  as a function of  $p_T$  (GeV/c), for four values of  $\sqrt{s}$  as indicated. Curves are the calculation of Ellis and Stirling with Duke-Owens set 1 structure functions,  $Q^2 = p_T^2$  and  $K = 2$ .

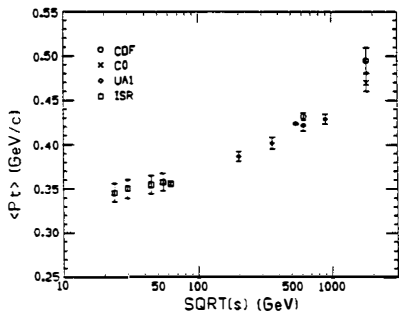


Fig. 3  $\langle p_T \rangle$  vs.  $\ln(\sqrt{s})$  for pp and  $\bar{p}p$  nondiffractive inelastic events, at ISR to TeVatron energies. An additional overall systematic error of  $\pm 20$  MeV/c common to the CDF points at 630 and 1800 GeV is omitted.

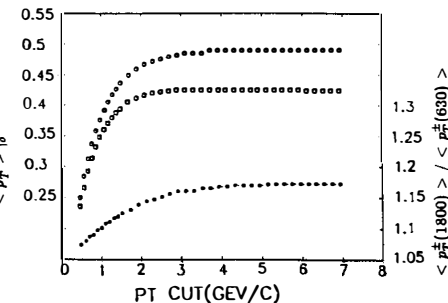


Fig. 4 (a)  $\langle p_T \rangle$  at 1800 and 630 GeV averaged over the charged particle momentum range from zero up to various values of  $p_T(\text{cut})$ . (b) (lower curve, right hand scale) The ratio of  $\langle p_T \rangle$  at 1800 GeV/630 GeV, vs  $p_T(\text{cut})$ .

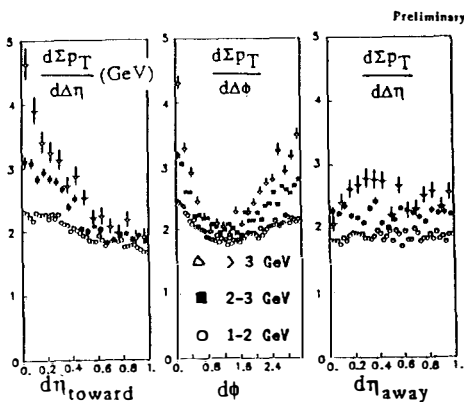


Fig. 5 Charged particle momentum flow densities around trigger particles of various  $p_T$ , for (a) same-side in  $\phi$  and (c) away-side in  $\phi$  as a function of distance in  $\eta$  from trigger particle; (b) as a function of distance in  $\phi$  from trigger particle.

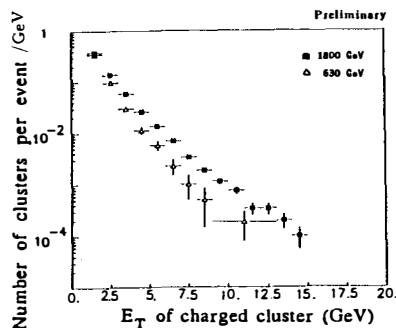


Fig. 6 Charged cluster  $E_T$  spectrum for 630 and 1800 GeV data, for  $-0.7 < y_{clus,ster} < 0.7$ .

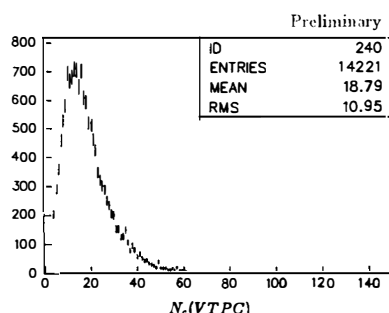
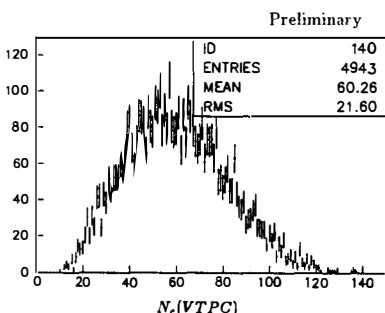


Fig. 7 (a) VTPC track multiplicity distribution for 3 GeV cluster events and (b) for non-1-GeV-cluster events; in 1.8 TeV minimum bias data.